

## Visualization of Dynamic Conformational Switching of the G-Quadruplex in a DNA Nanostructure

Yuta Sannohe,<sup>†</sup> Masayuki Endo,<sup>\*,‡,§</sup> Yousuke Katsuda,<sup>†</sup> Kumi Hidaka,<sup>†</sup> and Hiroshi Sugiyama<sup>\*,†,‡,§</sup>

Department of Chemistry, Graduate School of Science, Kyoto University, Kitashirakawa-oiwakecho, Sakyo-ku, Kyoto, 606-8502, Japan, Institute for Integrated Cell-Material Sciences (iCeMS), Kyoto University, Yoshida-ushinomiya-cho, Sakyo-ku, Kyoto 606-8501, Japan, and CREST, Japan Science and Technology Corporation (JST), Sanbancho, Chiyoda-ku, Tokyo 102-0075, Japan

Received July 4, 2010; E-mail: endo@kuchem.kyoto-u.ac.jp; hs@kuchem.kyoto-u.ac.jp

**Abstract:** We herein report the real-time observation of G-quadruplex formation by monitoring the G-quadruplex-induced global change of two duplexes incorporated in a DNA nanoscaffold. The introduced G-rich strands formed an interstrand (3 + 1) G-quadruplex structure in the presence of K<sup>+</sup>, and the formed four-stranded structure was disrupted by removal of K<sup>+</sup>. These conformational changes were visualized in a nanoscaffold in real-time with fast-scanning atomic force microscopy.

Conformational changes in the DNA of living systems are closely linked to the precise regulation of their biological functions, such as gene expression.<sup>1</sup> The formation of a four-stranded structure, the so-called G-quadruplex, is of great interest because of its structural variations and functions.<sup>2</sup> In connection with this, we have reported on a new, distant intrastrand quadruplex formation as a model structure in the human telomere region.<sup>3</sup> Moreover, we have recently proposed the folding pathways of human G-quadruplex structures.<sup>4</sup> Though the folding or the conformational changes of such a four-stranded structure was investigated by traditional spectroscopic methods, real-time observation has not yet been achieved.

In this study, we intended to directly observe the formation of single G-quadruplex structure under conditions that favors the folding of a four-strand structure and its disruption under unfavorable conditions. For this purpose, we employed a DNA nanoscaffold constructed using a DNA origami method.<sup>5</sup> We have recently developed a defined DNA scaffold, denoted as a “DNA frame” (Figure 1a), for visualization of the behavior of methyltransferase and repair enzymes bound to double-stranded DNA.<sup>6</sup> This frame contains an inner vacant rectangular area, in which two sets of connection sites (A–B and C–D) were introduced for the hybridization of duplex DNAs of interest. In order to place the G-rich sequences, we prepared two different unique DNA strands (G-strings) that contained the single-stranded terminal regions needed for the complementary base pairing with the DNA frame, and single-stranded G-rich overhangs at the middle for the formation of interstrand quadruplex (Figure 1a, Table S1). Three G-tracts of the sequence 5'-GGGTTAGGGTTAGGGTTT-3' were placed in the upper G-strand while the lower strand had a single G-tract of the sequence 5'-TTTGGGT-3'. In the absence of K<sup>+</sup>, the G-tracts will not fold into a four-stranded structure and hence the introduced strands will be parallel to each other (Figure 1b). On the other hand, in the presence of K<sup>+</sup>, the G-tracts are expected to fold into an

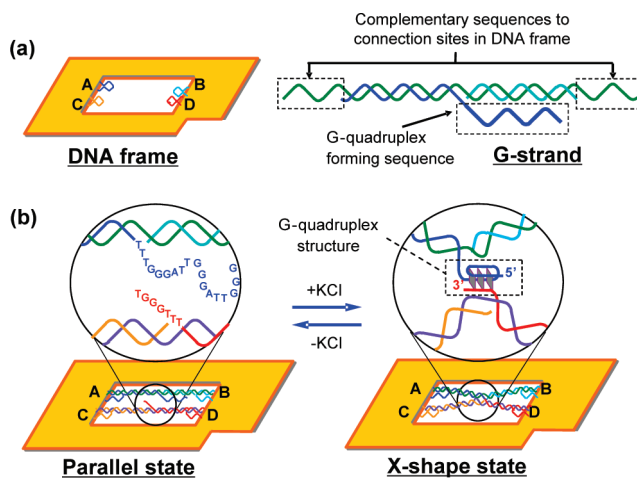


**Figure 1.** (a) Schematic representation of the DNA frame and G-strings. The DNA frame contains an inner vacant area in which four connection sites (A–D) are introduced for hybridization (left). The G-string contains a G-quadruplex-forming region and a DNA-frame hybridization region (right). (b) The DNA frame with G-strings forming the parallel state in the absence of K<sup>+</sup> (left) and the G-strings forming an “X” shape in the presence of K<sup>+</sup> due to the formation of a quadruplex structure.

interstrand quadruplex that will lead to the “X” shape of the strands introduced. This dynamic change in the DNA nanostructure can be monitored at the time scale and spatial resolution of fast-scanning atomic force microscopy (AFM).

We initially observed the conformation of the incorporated G-strings in a potassium-free buffer solution (Figure 2a and 2b). As we designed, these strands were parallel to each other and no contact or overlap between them was observed in this condition. In the presence of K<sup>+</sup>, however, the G-strings in the DNA frame clearly showed an “X” shape, which indicated the formation of an interstrand G-quadruplex (Figure 2c and 2d). About 35% of the G-strings in the DNA frame showed an “X” shape in the presence of K<sup>+</sup> (Table S2). The degree of flexibility of the G-strings is necessary for the formation of a quadruplex. Therefore, we extended the length of the G-strings from 64-mer to 74-mer to improve the efficiency of the formation of the “X” shape (Table S1). As we expected, the efficiency of the “X” shape formation was improved to 44%, after we replaced a shorter strand by a longer one (Figure S1, Table S2). Further, in order to confirm that the formation of “X” shape is exclusively attributed by the quadruplex, we investigated G-to-A mutated G-strings of the sequence 5'-GAGTTA-GAGTTAGAGTTT-3', which could not adopt a quadruplex structure (Table S1). None of the G-strings in the DNA frame showed an “X” shape in the presence of K<sup>+</sup>, which clearly indicated that the “X” shape is solely due to the formation of the G-

<sup>†</sup> Department of Chemistry, Kyoto University.

<sup>‡</sup> iCeMS, Kyoto University.

<sup>§</sup> CREST, JST.

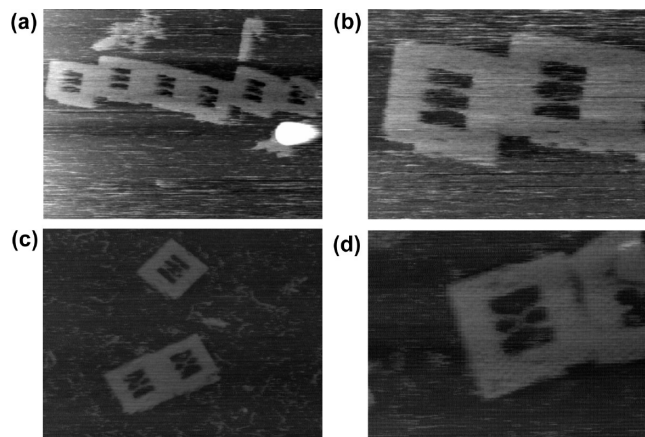


**Figure 2.** AFM images of a DNA frame containing G-strands. (a and b) DNA frames in the absence of  $K^+$ , (c and d) DNA frames in the presence of  $K^+$ . Image size =  $700 \times 525$  nm (a and c) and  $300 \times 225$  nm (b and d).

quadruplex (Figure S2). The static analysis described above indicated that our system is suitable to study the conformational changes from the unstructured single-stranded overhangs to a (3 + 1) interstand G-quadruplex.

Next, we aimed to directly observe the dynamic formation of a quadruplex in real time. A 64-mer upper G-strand containing three G-tracts and a 74-mer lower G-strand containing one G-tract was introduced into the DNA frame. The sample was prepared and adsorbed onto a freshly cleaved mica plate in the absence of  $K^+$ . After adding the observation buffer containing  $K^+$ , the sample was

scanned using fast-scanning AFM, which acquired one AFM image every 5 s. The results of the AFM scanning are summarized in Figure 3a. During scanning, the two G-strands maintained a parallel state for a given period, and then the G-strands suddenly formed an “X” shape (40 s in Figure 3a). This “X” shape remained unchanged and was not broken after the formation, indicating that the formed “X” shape is not due to the simple overlap of the strands. This result shows that the conformational change of the G-strands was captured in real time using this observation system, meaning that quadruplex formation had occurred during the successive AFM scanning. In some of the images obtained for the parallel state, the G-strands were not clearly visible. This could be due to the strong motion of these strands within the DNA frame. In contrast, the “X” shape is clearly visible throughout the AFM scanning, due to the fact that the motion of the G-strands was restricted by the formation of the quadruplex structure. Our results indicate that the quadruplex folding event is complete within the period of 5 s which is in close proximity to 0.2 s, the result obtained by stopped-flow experiments.<sup>7</sup> Note that the AFM scanning was carried out at a speed of one image every 5 s, and hence a better proximity to the experimental data is difficult to obtain at present. However, it is obvious to expect that the folding rate of the interstand quadruplex structure in the frame (where two G-strands are firmly fixed) is slower than the one obtained in bulk solution (where the G-strands will have translational degrees of freedom), because the probability of finding a strand crossing over the other is higher in the case of solution.

In a similar fashion, we tried to follow the disruption of the quadruplex in the absence of  $K^+$ . The “X” shape structure was

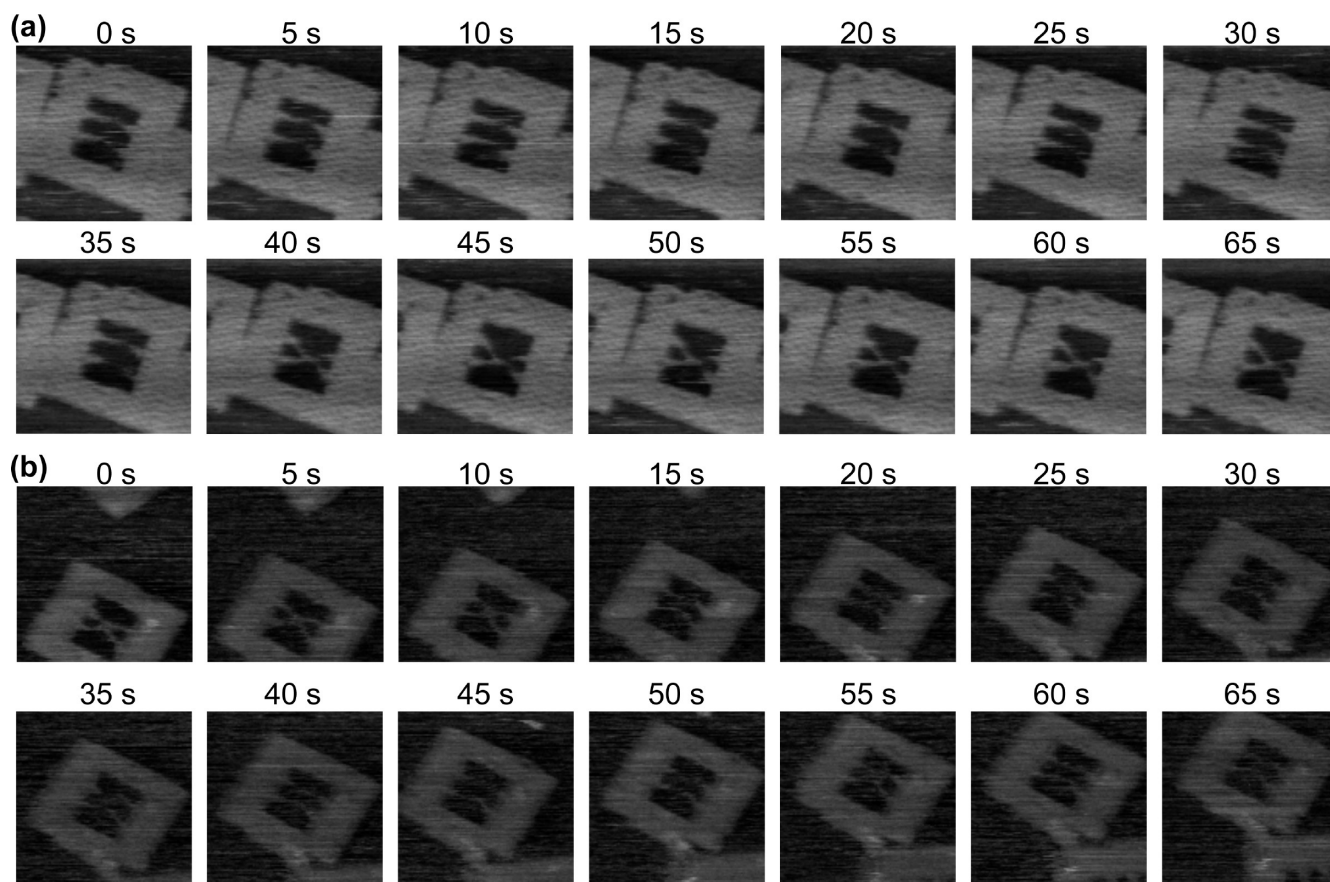


**Figure 3.** Successive fast-scanning AFM images of G-quadruplex formation/disruption events. (a) The formation of a quadruplex obtained at 5 s intervals, and (b) the disruption of a quadruplex obtained at 5 s intervals. Image size =  $160 \times 160$  (a) and  $175 \times 175$  nm (b).

formed in the presence of  $K^+$ . The sample was placed on a mica surface and soaked in the observation buffer without KCl (Figure 3b). The “X” shape remained unchanged for a while, and then it was reverted to the parallel state. Once the quadruplex structure dissociated, the parallel state did not form an “X” shape. This result suggests that  $K^+$  ions were released from the G-quadruplex structure, and these ions could not return to the G-strands after the interstrand quadruplex was disrupted.

Finally, we investigated the quadruplex formation with different conditions and sequences. To date, various interstrand G-quadruplex structures have been reported in human telomere sequences.<sup>8</sup> These structures are known to be highly influenced by sequences.<sup>4,9,10</sup> Therefore, we investigated different G-strands that contained two G-tracts, GGGTTAGGGTTT, in both the 64-mer upper strand and the 74-mer lower strands (Table S1). In this case, the strands in the DNA frame showed an “X” shape, which is comparable with the above results (Figure S3). In addition, cations are known to affect the formation of a G-quadruplex structure.<sup>11</sup> Thus, observations of a quadruplex structure in a buffer containing sodium ions as well as a potassium-containing buffer were carried out (Figure S4). In all cases, the DNA frame showed an “X” shape formation, even though the structure of the quadruplex was different. The formation ratios of the parallel and “X” shapes are summarized in Table S2. These results indicate that “X” shape formation is independent of the structure of the G-quadruplex. Therefore, our observation system using DNA nanostructures can be applied to various quadruplex structures.

We have successfully investigated the dynamics of the formation and disruption of G-quadruplexes by monitoring the changes in the DNA nanostructure by a high-speed AFM scanning system. It is noteworthy that this is the first report on the real-time observation of a reversible conformational change of a DNA. A large number of studies have been carried out on DNA-based nanomechanical machines since the DNA machine based on the B–Z conformational transition was reported.<sup>12</sup> Moreover, the formation of a G-quadruplex was applied for applications such as the induction of nanoparticle aggregation.<sup>13</sup> We anticipate that our primary results

could pave the way for the direct observation of various conformational changes known in nucleic acids.

**Acknowledgment.** We thank Dr. Arivazhagan Rajendran for critically reading the manuscript. This work was supported by Core Research for Evolutional Science and Technology (CREST) of JST and Grant-in-Aid for Science research from the MEXT, Japan. Sumitomo foundation to M.E. is also acknowledged.

**Supporting Information Available:** Experimental procedures, additional AFM images, sequences of oligonucleotides, and ratio of parallel and X-shape formation. This material is available free of charge via the Internet at <http://pubs.acs.org>.

## References

- (1) (a) Bacolla, A.; Wells, R. D. *J. Biol. Chem.* **2004**, *279*, 47411–47414. (b) Wells, R. D. *Trends Biochem. Sci.* **2007**, *32*, 271–278. (c) Bacolla, A.; Wells, R. D. *Mol. Carcinog.* **2009**, *48*, 273–285. (d) Zhao, J.; Bacolla, A.; Wang, G.; Vasquez, K. M. *Cell. Mol. Life Sci.* **2010**, *67*, 43–62. (e) Rajendran, A.; Nakano, S.; Sugimoto, N. *Chem. Commun.* **2010**, *46*, 1299–1301.
- (2) (a) Patel, D. J.; Phan, A. T.; Kuryavyi, V. *Nucleic Acids Res.* **2007**, *35*, 7429–7455. (b) Lipps, H. J.; Rhodes, D. *Trends Cell Biol.* **2009**, *19*, 414–422. (c) Sannohe, Y.; Sugiyama, H. *Curr. Protoc. Nucleic Acid Chem.* **2010**, *40*, 17.2.117.2.17.
- (3) Xu, Y.; Sato, H.; Sannohe, Y.; Shinohara, K.; Sugiyama, H. *J. Am. Chem. Soc.* **2008**, *130*, 16470–16471.
- (4) Mashimo, T.; Yagi, H.; Sannohe, Y.; Rajendran, A.; Sugiyama, H. *J. Am. Chem. Soc.* **2010**, *132*, 14910–14918.
- (5) Rothmund, P. W. *Nature* **2006**, *440*, 297–302.
- (6) (a) Endo, M.; Katsuda, Y.; Hidaka, K.; Sugiyama, H. *J. Am. Chem. Soc.* **2010**, *132*, 1592–1597. (b) Endo, M.; Katsuda, Y.; Hidaka, K.; Sugiyama, H. *Angew. Chem., Int. Ed.*, in press.
- (7) Gray, R. D.; Chaires, J. B. *Nucleic Acids Res.* **2008**, *36*, 4191–4203.
- (8) Dai, J.; Carver, M.; Yang, D. *Biochimie* **2008**, *90*, 1172–1183.
- (9) Zhang, N.; Phan, A. T.; Patel, D. J. *J. Am. Chem. Soc.* **2005**, *127*, 17277–17285.
- (10) Phan, A. T.; Patel, D. J. *J. Am. Chem. Soc.* **2003**, *125*, 15021–15027.
- (11) (a) Wang, Y.; Patel, D. J. *Structure* **1993**, *1*, 263–282. (b) Ambrus, A.; Chen, D.; Dai, J.; Bialis, T.; Jones, R. A.; Yang, D. *Nucleic Acids Res.* **2006**, *34*, 2723–2735. (c) Luu, K. N.; Phan, A. T.; Kuryavyi, V.; Lacroix, L.; Patel, D. J. *J. Am. Chem. Soc.* **2006**, *128*, 9963–9970. (d) Xu, Y.; Noguchi, Y.; Sugiyama, H. *Bioorg. Med. Chem.* **2006**, *14*, 5584–5591.
- (12) (a) Mao, C.; Sun, W.; Shen, Z.; Seeman, N. C. *Nature* **1999**, *397*, 144–146. (b) Liu, H.; Liu, D. *Chem. Commun.* **2009**, *19*, 2625–2636.
- (13) Li, Z.; Mirkin, C. A. *J. Am. Chem. Soc.* **2005**, *127*, 11568–11569.

JA1058907